Inverse photoemission spectroscopy at metal/acetonitrile interface by hole injection through solution species

Jiangbo Ouyang, and Allen J. Bard

J. Phys. Chem., **1988**, 92 (18), 5201-5205 • DOI: 10.1021/j100329a028

An Arrhenius plot of the rate constants k (inset of Figure 6) yields an activation energy for the dissolution of TiO_2 colloid (P1) of $E_a = 58 \pm 4$ kJ mol^{-1}. From the observation that the spectrum decays but does not blue-shift, we conclude that the rate-determining step of this dissolution is the initial attack of the crystallites by protons. Further degradation of smaller particles appears to proceed quickly. It is interesting to note that TiO_2 powder (P25, 2.5×10^{-4} M) does not dissolve at pH 1, even under drastic conditions (i.e., refluxing for 3 h).

Figure 7 shows the oxidation of iodide by photogenerated holes in air-saturated suspensions of TiO_2 colloids (P1 and P2) that have been illuminated with 5 mM photons at 330 nm. Quantum yields for the oxidation are given as a function of pH. As is obvious from the plot oxidation of I^- (eq 15) occurs only in the acid pH

$$I^- \xrightarrow[\Phi]{h\nu_b^+} I\cdot \qquad (15)$$

domain. Virtually no iodine or iodate is formed at pH >7. We conclude that I^- has to be adsorbed to the positively charged surface such that efficient hole scavenging can occur. The quantum yields shown in Figure 7 compare with a value of ≈2% reported previously by Herrmann and Pichat,[38] who illuminated a suspension of P25 TiO_2 powder at pH 0 ($[I^-] = 10$ mM) with UV light (300–400 nm); note, however, that at the low pH of their study the rate of the homogeneous oxidation of I^- (i.e., without TiO_2) is considerable (cf. Figure 7).

(38) Herrmann, J.-M.; Pichat, P. *J. Chem. Soc., Faraday Trans. 1* **1980**, *76*, 1138.

Summary

We have shown that controlled hydrolysis of $TiCl_4$ yields extremely small quantum-size TiO_2 particles ($d < 3$ nm, pH_{zpc} 5.1 ± 0.2) that possess anatase structure when prepared in aqueous solution. Excess negative charges created either by charge injection into the conduction band or by deprotonated surface hydroxyl groups lead to a blue-shift in the optical absorption spectrum of the transparent colloidal solution, which is understood in terms of an electrostatic model. Bandgap illumination of the semiconducting material results in the formation of blue Ti^{3+} centers under anoxic conditions with a quantum yield of 3%. The photocatalytic properties of the particles have been further demonstrated by the oxidation of I^-; the marked pH dependence of the quantum yield of this process reveals that surface adsorption of iodide ions is a prerequisite for iodine formation.

Acknowledgment. We are grateful for the assistance of M. Weller (HMI), Carol Garland (CIT), and K. Weiss (Fritz-Haber-Institut, Berlin) during the electron microscopic studies. D.W.B. thanks Prof. A. Henglein (HMI) and the Hahn-Meitner Institut for granting him a leave of absence. We extend our appreciation to G. Mills for helpful discussions and useful criticism. Financial support was provided by the U.S. EPA (R81162-01-0).

Registry No. TiO_2, 13463-67-7; HCl, 7647-01-0; I^-, 20461-54-5; $TiCl_4$, 7550-45-0; Ti, 7440-32-6.

Inverse Photoemission Spectroscopy at Metal/Acetonitrile Interface by Hole Injection through Solution Species

Jiangbo Ouyang and Allen J. Bard*

Department of Chemistry, The University of Texas, Austin, Texas 78712 *(Received: December 21, 1987)*

A series of compounds with standard potentials ranging from +0.22 to +1.44 V vs SCE were used for inverse photoemission spectroscopy (IPS) studies at the Pt/MeCN interface. Only those couples with standard potentials more positive than +1.0 (±0.1) V vs SCE produced inverse photoemission. For species generating emission, the more positive the standard potential, the greater the blue shift in the emission spectra. The wavelength and intensity of the emission spectra also depended on the cathodic limit of the potential pulse. As compared to a Pt electrode, a Rh electrode showed different IPS threshold potentials and weaker IPS emission with electron injection from benzophenone radical anion.

Introduction

We report here an investigation of inverse photoemission (IP) from a Pt electrode/MeCN electrolyte solution interface by hole injection from species produced from redox couples spanning the potential range +0.22 to +1.44 V vs SCE. We also compare IP at Pt and Rh electrodes by electron injection. Photoluminescence from a metal was reported by Mooradian[1] in 1969. McIntyre, Sass, and co-workers[2-5] first reported IP at a metal/solution interface by electrogeneration of a solution species which can inject a hole or electron into the electrode. For example, IP occurs upon generation of a radical cation, $D^{\cdot+}$, at a potential near its redox level, E°. When this species is reduced at a sufficiently negative potential, emission can be produced by radiative transitions in the metal, as illustrated in Figure 1. In a previous study[6] we reported IP produced by electron injection by a series of radical anions with redox potentials spanning a range of −0.60 to −2.22 V and demonstrated that only species with a potential more negative than a certain threshold level were capable of producing IP. We proposed a model for IP at the Pt/MeCN interface in which surface states promote radiationless processes at the interface. We also carried out experiments to eliminate the possibility that the observed emission is attributable to solution chemiluminescence reactions of impurities or background processes in MeCN. These previous studies suggest that inverse photoemission spectroscopy (IPS) is a useful technique for in situ studies of electrodes and for probing empty and occupied electronic states in the interfacial region.[6] The results presented in this paper complement our earlier study by investigating hole injection over a range of potentials and suggest how the combined results can be used to estimate the

(1) Mooradian, A. *Phys. Rev. Lett.* **1969**, *22*, 185.
(2) McIntyre, R.; Sass, J. K. *J. Electroanal. Chem.* **1985**, *196*, 199.
(3) McIntyre, R.; Sass, J. K. *Phys. Rev. Lett.* **1986**, *56*, 651.
(4) McIntyre, R.; Roe, D. K.; Sass, J. K.; Storck, W. *J. Electroanal. Chem.* **1987**, *228*, 293.
(5) McIntyre, R.; Roe, D. K.; Sass, J. K.; Gerischer, H. *Ber. Bunsen-Ges. Phys. Chem.* **1987**, *91*, 488.

(6) Ouyang, J.; Bard, A. J. *J. Phys. Chem.* **1987**, *91*, 4058.

0022-3654/88/2092-5201$01.50/0

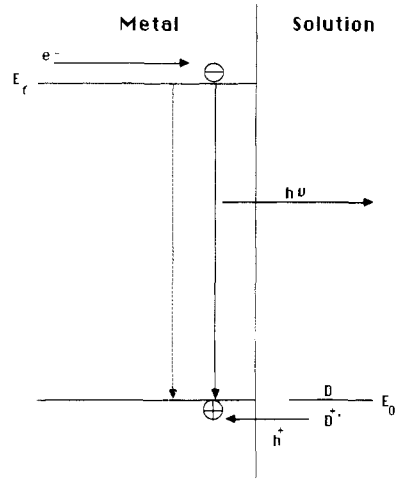

Figure 1. Model showing hole injection from a highly oxidizing species into a negatively biased metal electrode.

energy width covered by surface states at the interface.

Experimental Section

HPLC grade acetonitrile (Fisher Scientific Co., Fair Lawn, NJ) was purified and dried by continuous refluxing and then distillation from P_2O_5 under nitrogen. The solvent was further dried and degassed by three vacuum distillations over dry P_2O_5 and stored over Super 1 Woelm alumina N. Electrometric grade tetrabutylammonium tetrafluoroborate ((TBA)BF_4) (Southwestern Analytical Chemical Co., Austin, TX) was recrystallized 3 times from ethyl acetate and then dried in a vacuum oven at 85–100 °C for 36 h. All redox species were purified by literature methods.[9]

Cyclic voltammetric (CV) and inverse photoemission (IP) experiments were performed with a Princeton Applied Research (PAR) Model 175 universal programmer, Model 173 potentiostat/galvanostat, and Model 179 digital coulometer. A BAS 100 (Bioanalytical Systems, West Lafayette, IN) electrochemical analyzer was used to generate the normal pulse polarography potential wave form in the measurement of IP intensity–potential relations. The IP intensity vs potential curves were measured through the optical window of the electrochemical cell with a Hamamatsu Model R928 photomultiplier tube (PMT) (available range ca. 200–900 nm). A Nicolet Model 1090A digital oscilloscope was used to record the photomultiplier tube output during the double potential pulse. A one-compartment electrochemical cell was used in the experiment. The platinum working electrodes were either a polycrystalline platinum foil electrode or an electrode made from a 1000-Å-thick platinum film sputtered on a mica substrate.[10] For comparison, a Rh foil electrode was also used as working electrode. The cell also contained a Pt wire auxiliary electrode and an Ag wire quasi-reference electrode (AgRE). All potentials were referenced to the saturated calomel electrode (SCE) by observation of the voltammetry of ferrocene in the test solution after a series of IPS experiments. Solutions were prepared by transferring solvent under vacuum into the electrochemical cell containing purified and predried supporting electrolyte and redox species.

IP spectra were taken with a Model C1230 single-photon-counting system (Hamamatsu Corp., Bridgewater, NJ) utilizing a Hamamatsu R928P PMT, cooled to −25 °C in a Model TE 308 TSRF cooler controller (Products for Research Inc., Danvers, MA). A lens was used to focus the emission at the electrode onto the inlet slit of the spectrometer to minimize any loss in light intensity. The spectra were obtained point by point as the average of the emission intensities at each wavelength (with a set of 16 narrow-band interference filters) (Oriel, Stratford, CT); the emission intensity reported is the average of 8–10 measurements at each wavelength.

TABLE I: Inverse Photoemission by Hole Injection[a]

redox couple	$E°$, V vs SCE	detection of light	E_{th}, V vs SCE	E_T,[b] eV
TTF	0.22	no		
ferrocene	0.35	no		
phenothiazine	0.52	no		
acetylferrocene	0.60	no		
ferrocenecarboxylic acid	0.71	no		
1,1′-diacetylferrocene	0.86	no		
thianthrene	1.10	yes	−1.0	2.58
triphenylamine	1.10	yes	−1.0	3.04
tris(2,4-dibromophenyl)amine	1.43	yes	−0.5	*c*
9,10-dibromoanthracene	1.44	yes	−0.5	1.8

[a] The potential was pulsed between +1.6 and −1.3 V vs SCE, and the pulse width was 20 ms. [b] E_T is the energy of the triplet state. [c] Not available.

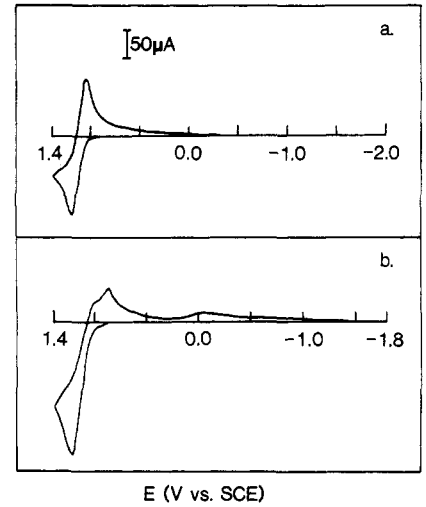

Figure 2. Cyclic voltammetric curves: (a) a saturated solution of thianthrene in acetonitrile/0.1 M (TBA)BF_4; (b) 20 mM triphenylamine in acetonitrile/(TBA)BF_4. The working electrode is Pt/mica. Scan rate = 100 mV/s.

Results

The IPS experiments reported here followed the hole injection model, employed by McIntyre, Sass, and co-workers[2-4] with thianthrene solutions, with a number of different radical ion precursors, D. In the experiment the potential is first stepped positive of the redox potential of the $D^{\bullet+}/D$ couple ($E°$) to generate $D^{\bullet+}$ at the electrode surface and then stepped to various more negative potentials until emission (within the wavelength range of the PMT) is observed. Following the definitions in our previous paper,[5] we define E_{th} as the threshold potential for emission. At any given potential more negative than E_{th}, an IP spectrum can be recorded. The shortest wavelength (highest energy) of the emission at a given applied potential is the threshold energy, ϵ_{th}. A series of different precursors, with different $E°$'s, were employed. For redox couples with $E°$'s less positive than a given value, no emission was observed for potential steps to the cathodic solvent limit. We denote this redox threshold as $E_{0,th}$.

Cyclic Voltammetry. Ten compounds, listed in Table I, with standard potentials (estimated from the CV E_p values) ranging from +0.22 to +1.44 V vs SCE were used. These were selected because they form reasonably stable radical cations and do not luminesce strongly in the visible region. Except for triphenylamine, all other redox couples showed reversible cyclic voltammetric waves for oxidation at a scan rate of 100 mV/s. The oxidation of triphenylamine showed only a small cathodic peak on the reverse scan, as well as a reversible cyclic voltammetric wave attributable

(7) Smith, N. V.; Woodruff, D. P. *Prog. Surf. Sci.* **1986**, *21*, 295.
(8) Ouyang, J.; Bard, A. J. *J. Electroanal. Chem.* **1987**, *222*, 331.
(9) Perrin, D. D.; Armarego, W. L. F.; Perrin, D. R. *Purification of Laboratory Chemicals*, 2nd ed.; Pergamon: New York, 1981.
(10) Liu, H. Y.; Fan, F.-R. F.; Bard, A. J. *J. Electrochem. Soc.* **1985**, *132*, 2666.

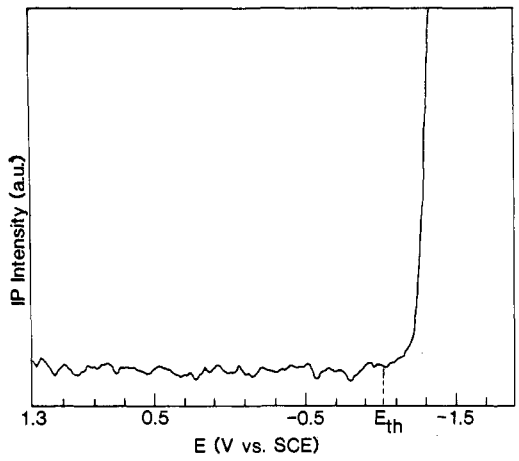

Figure 3. Emission intensity–potential profile for a saturated solution of thianthrene in acetonitrile/(TBA)BF_4. The emission is the unfiltered response of the photomultiplier tube.

to a dimeric product of the radical cation (Figure 2).[11] Despite this complication, triphenylamine is included in this study, since the oxidation potential of triphenylamine is the same as thianthrene and both redox couples showed the same threshold potential.

Observation of Inverse Photoemission and Threshold Potential. The cation radicals were generated by a potential step positive of the oxidation peak potential of the redox species used. A pulse width of 20 ms was usually employed. The cation radicals were then reduced at a potential which was stepped to progressively more negative potentials. A scan rate of 100 mV/s was used, and the potential difference per step was 4 mV. The emission intensity was recorded as a function of the scanning potential. The emission time response were generally the same as those reported previously (see Figure 6 in ref 6). Figure 3 shows a typical emission intensity–potential profile for a saturated solution of thianthrene in MeCN/0.1 M (TBA)BF_4 at a Pt electrode. Three other compounds, triphenylamine, tris(2,4-dibromophenyl)amine, and 9,10-dibromoanthracene, showed emission and similar intensity–potential profiles. The other compounds (TTF, ferrocene, phenothiazine, ferrocenecarboxylic acid, acetylferrocene, and 1,1′-diacetylferrocene) did not show emission even when the potential was stepped to −2.5 V vs SCE (close to the MeCN background reduction). Species with $E°$'s equal to or positive of +1.10 V vs SCE produced IPS while those with $E°$'s less positive than +0.86 V vs SCE did not. We thus place $E_{0,th}$ at +1.0 (±0.1) V vs SCE. For those redox species which do give rise to IP, the final negative pulse potential must reach a threshold value, E_{th}, for the onset of IP (total emission <900 nm). The threshold potentials were determined from the emission intensity–potential profiles, such as that in Figure 3, and are listed in Table I.

Double potential step experiments were also conducted to eliminate the possibility that emission was due to a solution-phase process (e.g., reaction of radical cation with impurities or an electrogenerated reductant). The potential step sequence, first positive of the peak oxidation potential and then negative of the threshold potential, E_{th}, was essential for the generation of IP. The opposite potential step sequence, negative first and then positive, did not give rise to IP. Thianthrene would generate emission only upon the oxidation if the solvent was not freshly purified. Therefore, care was taken when thianthrene was used to ensure that the direct oxidation of thianthrene would not produce emission in each IPS experiment.

IP spectra were obtained for thianthrene and tris(2,4-dibromophenyl)amine with continuous potential pulsing between +1.6 and −1.3 V vs SCE. As shown in Figure 4, the spectra were in the visible region (between 430 and 800 nm). The peak intensities occurred at about 600 nm, with a ϵ_{th} near 420 nm (3.0 eV), close to that expected from the applied potential. The IP

(11) Vettorazzi, N.; Silber, J. J.; Seveno, L. *J. Electroanal. Chem.* **1985**, *158*, 89.

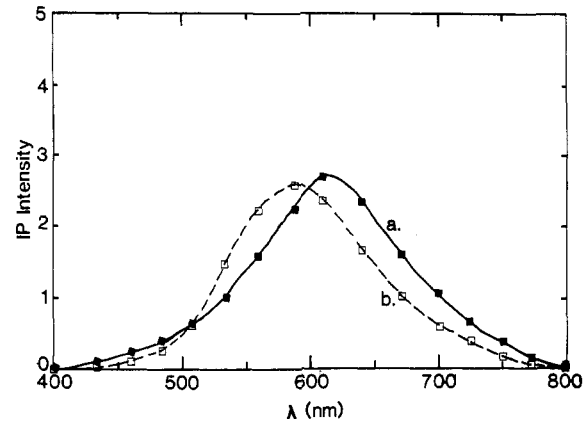

Figure 4. Inverse photoemission spectra for (a) thianthrene (the intensity axis is 1000 counts per unit) and (b) tris(2,4-dibromophenyl)amine (the intensity axis is 2000 counts per unit). The working electrode is platinum, and the potential pulses are between +1.6 and −1.3 V vs SCE. Points are the average of 10 measurements at each wavelength.

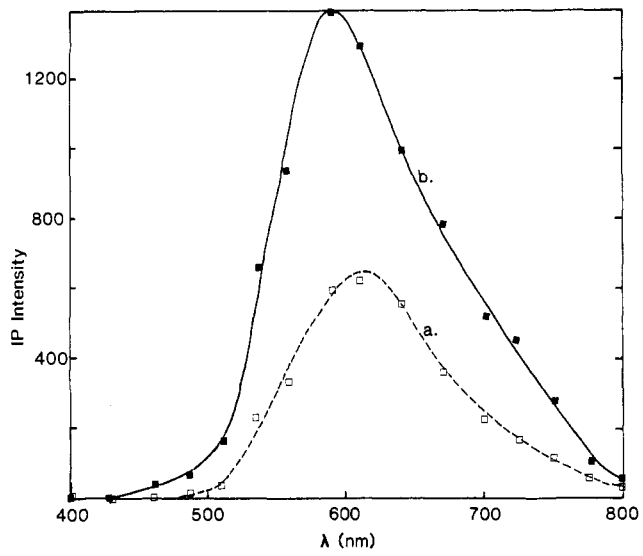

Figure 5. Potential dependence of inverse photoemission spectra for a saturated solution of tris(2,4-dibromophenyl)amine in MeCN/0.1 M (TBA)BF_4. Platinum is the working electrode. The potential is pulsed (a) between +1.6 and −1.0 V vs SCE and (b) between +1.6 and −1.3 V vs SCE.

spectrum of thianthrene found here was similar to that reported for that on Au(111) by McIntyre and Sass.[2] The IP spectrum of tris(2,4-dibromophenyl)amine showed a slight blue shift relative to that of thianthrene. The spectra were taken point by point, averaging the intensities at each different wavelength. The emissions for 9,10-dibromoanthracene and triphenylamine were also in the visible region, but reliable IP spectra could not be obtained. The cyclic voltammetric wave of 9,10-dibromoanthracene showed an irreversible reduction peak at −1.3 V vs SCE. The oxidation of triphenylamine was followed by a dimerization process. In both cases prolonged potential pulsing degraded the solutions and decreased the emission intensity.

IP spectra were also recorded with tris(2,4-dibromophenyl)amine by pulsing the potential to different lower limits. Figure 5a shows the IP spectrum obtained with potential pulsing between +1.60 and −1.0 V vs SCE, and Figure 5b shows that with pulsing between +1.60 and −1.3 V. Note that the IP spectrum was shifted slightly to higher energy as the lower limit of the pulsing potential was changed from −1.0 to −1.3 V vs SCE, with ϵ_{th} changing from 2.6 to 2.9 eV.

IPS Emission from Rh Electrode. IP at a Rh electrode differs from that at Pt, demonstrating that the emission originates in the metal and not in electrogenerated products in solution. In Figure 6 are shown the IPS intensity–potential profiles of 50 mM benzophenone at a Pt electrode (Figure 6a) and at a Rh electrode

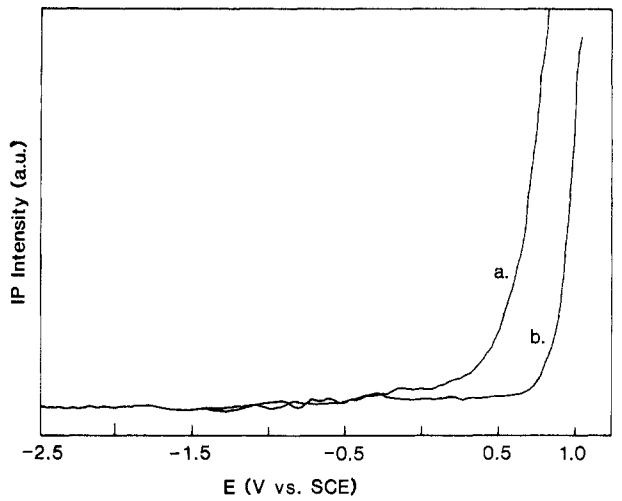

Figure 6. Emission intensity–potential profiles for 50 mM benzophenone in MeCN/0.1 M (TBA)BF_4: (a) Pt as working electrode; (b) Rh as working electrode.

(Figure 6b). With the same configurations of the electrochemical and light detection systems, the emission intensity from the Rh electrode normalized to electrode area was about 5 times smaller than that from the Pt electrode. The threshold potential to produce IPS emission at the Rh electrode was shifted to +0.7 V from the +0.2 V at a Pt electrode.

Discussion

The results presented here support the original findings of McIntyre and Sass[2,3] and yield additional evidence that electrochemical generation of IP occurs and that the observed weak emission is not a solution chemiluminescent process. A series of nonluminescent or weakly luminescent substances were chosen for this study. The potential range used was within the oxidation and reduction limits of MeCN/0.1 M (TBA)BF_4 to avoid the generation of background ECL.[6] It is unlikely that the emission is due to an ECL process of an annihilation type. The observation of emission depended on the energy level (as represented by the standard redox potential) of the redox couple used, rather than its chemical nature. Thianthrene has a different structure and luminescence properties than triphenylamine, yet the threshold potentials to obtain emission were the same (−1.0 V vs SCE) for both redox couples, as they have the same standard potential for oxidation (+1.10 V vs SCE). Tris(2,4-dibromophenyl)amine and 9,10-dibromoanthracene are another pair of redox couples that differ in luminescence properties and structure but show the same threshold potential (−0.50 V vs SCE) for emission and have similar standard potentials (+1.44 V vs SCE). The double potential step studies also show that the emission is not an ECL process. Only when the potential was first stepped to a positive value, where the redox species were oxidized, and then to a negative threshold value was emission observed. The opposite potential sequence (first negative and then positive) did not give rise to emission.

Moreover, the emission spectra for thianthrene and tris(2,4-dibromophenyl)amine are similar, not related to the emission spectra of the compounds, and are functions of the applied potential steps. These findings are consistent with the model for IPS at a metal/electrolyte solution interface.[3-5] The value of ϵ_{th} agreed with the magnitude of applied potential, i.e., with the cathodic limit at which the oxidized species is reduced. For the system Pt/MeCN, 0.1 M (TBA)BF_4, tris(2,4-dibromophenyl)-amine, when the potential was pulsed between +1.6 and −1.0 V vs SCE, the shortest wavelength of emission (threshold energy, ϵ_{th}) was 485 nm (2.56 eV), while ϵ_{th} was 430 nm (2.88 eV) when the potential was pulsed between +1.6 and −1.3 V vs SCE. Additional evidence that the emission was not a solution ECL process is the lower emission intensity and different value of E_{th} at a Rh electrode compared to those at a Pt electrode. The lower emission intensity from Rh found in the present study is consistent with a lower photoluminescence intensity from Rh than from Pt.[12]

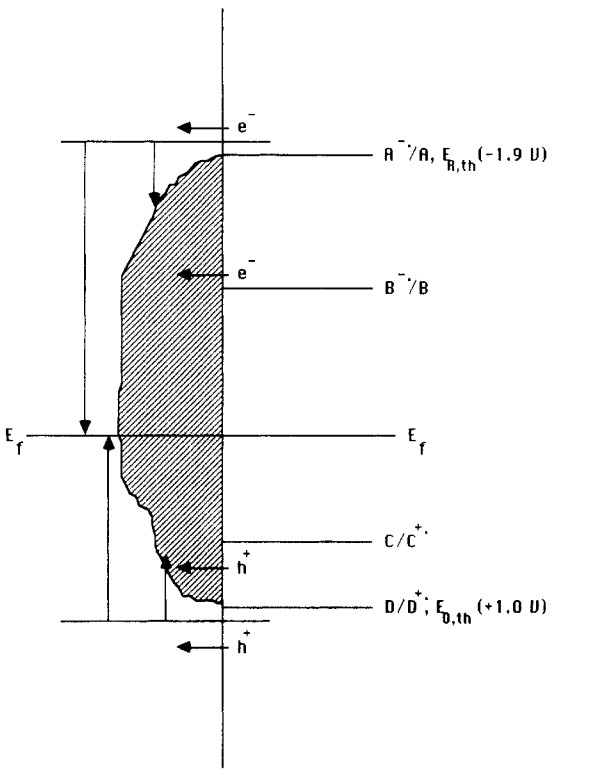

Figure 7. Energy level diagram depicting inverse photoemission processes at Pt electrode/MeCN solution interface.

Note that IPS has also been reported with Au(111) and stress-annealed pyrolytic graphite electrodes by reduction of the thianthrene cation radical.[2,3]

The mechanism of IP is consistent with the hole injection model previously proposed for thianthrene[2-4] and illustrated in Figure 7. Oxidation of D to D^+, followed by a cathodic pulse to a sufficiently negative potential, E_{th}, leads to injection of a hole (h^+) at an energy near $E°_{D^+/D}$ and an electron (e^-) at E_{th}. Both radiative and nonradiative combinations of h^+ and e^- occur. Because of the strong electron/hole–lattice interaction, the radiative transition is very weak, which accounts for the low IPS intensity.[13] Note that analogous processes involving e^- injection by radical anions (shown in Figure 7 as $A^{\bullet-}$) also occur.[1,5]

A novel aspect of this investigation is the observation of a redox threshold, $E_{0,th}$, for radical cation h^+ injection, which parallels IPS production by e^- injection at a Pt/MeCN interface with several redox couples with standard reduction potentials ranging from −0.60 and −2.22 V vs SCE. A redox threshold, $E_{R,th}$, was introduced[6] to account for the observation that the energy of the injected electron (proportional to the standard redox potential of a redox couple) had to be above a certain level for IP to occur. The existence of the redox threshold was attributed to a Shockley-type surface state on the electrode surface that promotes nonradiative recombination of the e^-h^+ pair. We find here that only those redox species with standard potential for oxidation more positive than +1.0 (±0.1) V vs SCE produce emission. This introduces another redox threshold, $E_{0,th}$, and suggests, as shown in Figure 7, a distribution of surface states of energies in a region corresponding to potentials more negative than $E_{0,th}$. Hole injection from a less positive couple (C^+/C) directly into these surface states should lead to more rapid radiationless decay. Only couples (D^+/D) below this level would inject holes that would lead to detectable emission. Previous experimental and theoretical studies[14-16] of metals have shown the existence of Shockley-type

(12) Shannon, C.; Campion, A., private communication.
(13) Pendry, J. B. *Phys. Rev. Lett.* **1980**, *45*, 1356.
(14) (a) Gartland, P. O.; Slagsvold, B. *Phys. Rev. B: Solid State* **1975**, *12*, 4047. (b) Nilsson, P. O.; Kanski, J.; Larsson, C. G. *Solid State Commun.* **1980**, *36*, 11.
(15) Hansson, G. V.; Flodstrom, S. A. *Phys. Rev. B: Solid State* **1978**, *17*, 473.

surface states. If this model is correct, the difference $E_{0,th}-E_{R,th}$ provides an estimate of the energy width covered by the surface states. For Pt/0.1 M (TBA)BF_4 in MeCN with $E_{R,th}$ of -1.90 V and $E_{0,th}$ of +1.0 V vs SCE, $E_{0,th} - E_{R,th}$ is 2.9 (±0.1) eV. This value has previously been estimated to be about 2-3 eV.[17]

Conclusions

In agreement with earlier studies,[1-5] IP occurs from a metal electrode by either hole or electron injection from a solution species; the emission cannot be attributed predominantly to electrogenerated chemiluminescence from solution reactions. By employing a series of redox couples with different standard potentials, one can probe surface states at the metal/solution interface. In this study of hole injection by radical cations we have found that only those redox couples with standard potentials more positive than +1.0 (±0.1) V vs SCE produce IP. From the difference of redox thresholds $E_{0,th}$ and $E_{R,th}$, we propose a distribution of states at Pt/MeCN over a region 2.9 (±0.1) eV in width, distributed from -1.90 to +1.0 V vs SCE.

Acknowledgment. The support of this research by the Army Research Office and the National Science Foundation (Grant CHE8304666) is gratefully acknowledged. We are indebted to Dr. Alan Campion for suggesting the use of the Rh electrode.

(16) Gurman, S. J. *J. Phys. C* **1979**, *9*, L609.
(17) Larsson, C. G.; Nilsson, P. O. *Phys. Lett. A* **1981**, *85A*, 393.

Reactions of Ethanethiol on Mo(110): Formation and Decomposition of a Surface Alkyl Thiolate

Jeffrey T. Roberts and C. M. Friend*

Department of Chemistry, Harvard University, Cambridge, Massachusetts 02138
(Received: December 29, 1987)

The reactions of ethanethiol (C_2H_5SH) on Mo(110) under ultrahigh vacuum have been investigated by temperature-programmed reaction, X-ray photoelectron, and high-resolution electron energy loss spectroscopies. Electron energy loss spectroscopy indicates that the S-H bond in ethanethiol dissociates below 120 K to form a surface ethyl thiolate (C_2H_5S). At low coverages the ethyl thiolate decomposes to atomic carbon, atomic sulfur, and gaseous H_2, with decomposition complete below 350 K. At high coverages, the surface thiolate decomposes during temperature-programmed reaction via three competing pathways: hydrogenolysis at 300 K to gaseous ethane, dehydrogenation at 340 K to gaseous ethylene, and decomposition to surface carbon, surface sulfur, and gaseous dihydrogen. Notably, the presence of surface atomic sulfur is *not* necessary for selective formation on clean Mo(110): the thiolate remains intact up to the temperature of hydrogenolysis onset. The last pathway proceeds via a hydrocarbon fragment(s) which decomposes at 570 K to gaseous H_2 and atomic carbon. At saturation, ≈75% of all irreversibly chemisorbed ethanethiol forms gaseous hydrocarbons. The coverage-dependent kinetics for ethanethiol decomposition are discussed in terms of electronic and site-blocking effects.

Introduction

The reactions of alcohols on single-crystal transition-metal surfaces have been the subject of much research.[1] Much less studied, however, are the reactions of thiols, the sulfur-containing analogues of organic alcohols.[2] The relatively weak C-S and S-H bonds in thiols might be expected to induce patterns in reactivity qualitatively different from those observed for alcohols. Thus, while the products from reaction of alcohols on transition-metal surfaces often have intact C-O bonds, the products of analogous thiols might be qualitatively different due to the weak C-S bond. Furthermore, desulfurization reactions of thiols are potentially important models for the related, technologically important hydrodesulfurization reactions.

In our previous work, we showed that the three-, four- and five-carbon thiols react on Mo(110) to produce the corresponding linear alkane and alkenes at high exposure. In all cases, the alkyl thiolate was proposed as the key surface intermediate that results in hydrocarbon formation. The alkene formation was proposed to proceed via selective dehydrogenation of the carbon β to the sulfur, which would yield the 1-alkene. The reaction kinetics and selectivity are dependent on exposure in all cases, with irreversible, nonselective decomposition predominating at low exposure. Furthermore, the kinetics for thiolate hydrogenolysis to form the alkane were shown to be essentially independent of alkyl chain length for the primary thiols, including the two-carbon ethanethiol.[2c]

This paper concerns the reactions of ethanethiol (C_2H_5SH) on Mo(110) and is part of the comprehensive study of alkyl thiols on Mo(110).[2a-e] We find that ethanethiol decomposes on Mo(110) to form ethane at 300 K and ethylene at ≈340 K. Another pathway, accounting for ≈25% of all chemisorbed ethanethiol, is decomposition to surface carbon, surface sulfur, and gaseous dihydrogen. The reactions of ethanethiol on Mo(110) are analogous to those of 1-propanethiol and 1-butanethiol, which also decompose to alkanes and alkenes between 300 and 400 K.[2a,b] This work specifically focuses on the identification and characterization of the ethyl thiolate and nonvolatile products formed from its reaction on Mo(110) using electron energy loss, temperature-programmed reaction, and X-ray photoelectron spectroscopies.

Experimental Section

The experiments reported here were performed in three ultrahigh-vacuum chambers, all of which have been described in detail previously.[2a,3,4] The working base pressure in each of the chambers

(1) (a) Miles, S. L.; Bernasek, S. L.; Gland, J. L. *J. Phys. Chem.* **1983**, *87*, 1626-1630. (b) Ko, E. I.; Madix, R. J. *Surf. Sci.* **1981**, *112*, 373-385. (c) Hrbek, J.; dePaola, R. A.; Hoffmann, F. M. *J. Chem. Phys.* **1984**, *81*, 2818-2827.
(2) (a) Roberts, J. T.; Friend, C. M. *J. Am. Chem. Soc.* **1986**, *108*, 7204-7210. (b) Roberts, J. T.; Friend, C. M. *J. Am. Chem. Soc.* **1987**, *109*, 3872-3882. (c) Roberts, J. T.; Friend, C. M. *J. Am. Chem. Soc.* **1987**, *109*, 4423-4424. (d) Roberts, J. T.; Friend, C. M. *J. Chem. Phys.*, in press. (e) Deleted in proof. (f) Preston, R. E.; Benziger, J. *J. Phys. Chem.* **1985**, *89*, 5010-5017. (g) Koestner, R. J.; Stohr, J.; Gland, J. L.; Kollin, E. B.; Sette, F. *Chem. Phys. Lett.* **1985**, *120*, 285-291. (h) Lang, J.; Masel, R. I. *Surf. Sci.* **1987**, *103*, 44-66. (i) Nuzzo, R.; Zegarski, B. R.; Dubois, L. H. *J. Am. Chem. Soc.* **1987**, *109*, 733-740.
(3) Baldwin, E. K.; Friend, C. M. *J. Phys. Chem.* **1985**, *89*, 2576-2581.
(4) Stuve, E. M.; Madix, R. J.; Brundle, C. R. *Surf. Sci.* **1984**, *146*, 155-178.

0022-3654/88/2092-5205$01.50/0